A model study of enhanced oil recovery by flooding with aqueous surfactant solution and comparison with theory.

Paul D.I. Fletcher*, Luke D. Savory and Freya Woods
Surfactant & Colloid Group, Department of Chemistry, University of Hull, Hull. HU6 7RX. U.K.
Andrew Clarke and Andrew M. Howe
Schlumberger Gould Research, High Cross, Madingley Road, Cambridge CB3 0EL

Electronic Supplementary Information

Characterisation of the calcite particles and the flow properties of packed columns.

As seen in Figure S1, the three calcium carbonate powders all consist of polydisperse, low axial ratio and irregularly shaped particles. The cumulative size distributions obtained by sieving analysis are shown in Figure S1 and the derived mean particle sizes from both sieving and SEM image analysis are given in Table 1. The BET measurements show the particles contain 4-8 vol% of internal pores with mean diameters ranging from 26 to 110 nm. In packed columns of the calcite powders, the interstitial volume fractions ϕ_{pore} are 0.34 for FC200, 0.40 for FC30 and 0.45 for FC10. This interstitial volume forms the network of interlinked pores (external to the particles) of varying dimensions within which oil is trapped in the packed columns and through which the pumped displacing liquids flow. The packed column pore volume fractions ϕ_{pore} are comparable to the interstitial space volume fractions of randomly close packed, monodisperse hard spheres which range from 0.40 to 0.36[1].

The flow properties of packed columns of the calcite particles of different sizes were investigated by flowing pure liquids through the packed columns at a set volumetric flow rate and recording the pressure drop between either pressure sensor 1 or 2 and the packed column exit. The upper plot of Figure S4a shows the variation of pressure drop as decane is pumped at a constant volumetric flow rate of 1 ml min^{-1} into an FC10 packed column initially filled with air. Initially, when the volume of decane pumped is less than the pore volume, the

pressure drop increases as the air in the packed column pores is displaced by the decane. Once all the air is displaced (when the decane pumped volume is equal to or greater than the packed column pore volume) the pressure drop required to maintain the volumetric flow rate is constant.

For packed columns filled with water, the upper graph of Figure S2 shows that the measured pressure drop is proportional to the volumetric water flow rate for packed columns containing the three calcite powders of different mean particle size and for a column containing no powder but including the frits shown in Figure 2. These plots demonstrate that Darcy's Law is obeyed for all the different systems over the range of pressure drops from 0 to approximately 18 MPa. The permeabilities increase in the order "empty" column (40×10^{-15} m^2 = 36 mD) > FC200 (20×10^{-15} m^2 = 21 mD) > FC30 (5.4×10^{-15} m^2 = 5.5 mD) > FC10 (1.2×10^{-15} m^2 =1.2 mD). The permeability value for the "empty" column includes the frits but the values quoted for the packed powders do not. This behaviour is expected since the volume fractions of the interstices between the packed calcite particles (the packed column pores) are similar for the different calcite powders but the average packed column pore sizes, and hence the permeabilities, are expected to decrease with decreasing calcite particle size. For the FC10 packed column, deviation from Darcy's Law is observed for volumetric flow rates greater than approximately 2 ml min^{-1} which require a pressure drop >18 MPa which we suggest may be due to the high pressure drop causing an increase in the packing density of the calcite powder in the column. Consistent with this hypothesis, it was seen that the FC10 packed column contained some empty space when the column was opened and examined following pumping at a pressure drop of 27 MPa (corresponding to the highest data point of the FC10 plot in the upper graph of Figure S2). In principle, an alternative explanation for this deviation could be a transition from laminar to turbulent flow at the high pressures. However, we estimate that the maximum value of Reynolds number in all systems tested is

approximately 10^{-6} and hence conclude that the deviation is due to packing changes at high pressures.

The data shown in Figure S2 can be used to estimate the mean packed column pore sizes for the calcite powders of different mean sizes. As seen in Figure S2, liquid flow in the packed columns follows Darcy's law which can be written as:

$$\Delta P = \frac{Q\mu L}{AK} \tag{S1}$$

where K is the permeability coefficient, ΔP is the pressure drop across the packed column, Q is the volumetric flow rate, μ is the fluid viscosity, L is the packed column length in the direction of the fluid flow and A is the overall packed column cross-sectional area. The permeability coefficient K of a packed column is expected to depend on the porosity, the average pore diameter and factors dependent on the detailed geometry of the pore network such as tortuosity and inter-connectivity. The results of pressure drop versus volumetric flow rate in Figure S2 can be used to estimate an *effective* average pore radius based on a hypothetical porous system which is hydrodynamically equivalent to the actual pore network present in a packed column. We consider a hypothetical system consisting of a cylindrical packed column containing a volume fraction ϕ_{pores} of uniform, cylindrical pores of radius r_{pore} aligned parallel to the flow direction[2]. The number of pores (n) in the packed column is

$$n = \frac{\phi_{pore} A}{\pi \cdot r_{pore}^2} \tag{S2}$$

Assuming the fluid flow through the cylindrical pores is laminar, the Hagen-Poiseuille equation yields the volumetric flow rate Q as:

$$Q = \frac{n\Delta P \pi \cdot r_{pore}^4}{8\mu L} \tag{S3}$$

Substituting for n in equation (S3) yields the final expression for the value of the *effective* (i.e. hydrodynamically equivalent) mean pore radius r_{pore} in terms of the measured values of ΔP as a function of Q.

$$r_{pore} = \sqrt{\frac{8Q\mu L}{\phi_{pore} A \Delta P}} \qquad \text{(S4)}$$

Using the data of Figure S2, the pressure drop across the packed column ΔP was obtained from the measured pressure drop by subtracting the corresponding pressure drop across the flow system and column containing no calcium carbonate powder. Equation S4 was then used to derive the values of r_{pore} for the three calcite powders which are summarised in Table 1.

Computer simulations[1] of the pore size distributions in random close packed, monodisperse, hard spheres for pore volume fractions in the range 0.3 to 0.4 show (i) that the mean pore radius r'_{pore} (based on the average radius of a particle which will insert at different points in the pore space) scales with the particle radius according to $r'_{pore} = k\ r_{particle}$, and (ii) that the scaling coefficient k increases with increasing pore volume fraction (mean $r'_{pore} \approx 0.14 \times r_{particle}$ for $\phi_{pore} = 0.3$ and mean $r'_{pore} \approx 0.24 \times r_{particle}$ for $\phi_{pore} = 0.4$). The FC10, FC30 and FC200 powders are polydisperse, irregularly shaped and close pack in the column with the different pore volume fractions shown in Table 1. If it is assumed that the mean (hydrodynamically-equivalent) pore radius r_{pore} of the calcite powder packed columns scales linearly with $r_{particle}$ despite their polydispersity and irregular shape (i.e. $r_{pore} = k\ r_{particle}$), it is expected that the results for the different powders will show different values of the scaling coefficient k because of the different values of ϕ_{pore}. As seen in the lower plot of Figure S2, the scaling coefficients estimated for the calcite powders range from 0.114 for $\phi_{pore} = 0.45$ to 0.030 for $\phi_{pore} = 0.34$, i.e. the packed calcite powders give mean pore radii which are approximately 4-fold smaller than monodisperse, spherical particles of the same radius which are randomly close packed at the same pore volume fraction. Two factors are likely to contribute to this difference. Firstly, the mean value of r'_{pore} in the computer simulations (based on the average size of particle which can be inserted into different points in the pore space) is not directly equivalent to the mean r_{pore} for the calcite powders which based on a

hydrodynamically equivalent pore radius. Secondly, the calcite particles are polydisperse and irregularly shaped, which seems likely to lead to a reduced value of mean pore radius relative to the monodisperse hard spheres used in the computer simulations.

References

1. Baranau, V.; Hlushkou, D.; Khirevich, S.; Tallarek, U. Pore-size entropy of random hard-sphere packings. *Soft Matter*, **2013**, *9*, 3361-3372.
2. Fletcher, P.D.I.; Haswell, S.J.; He, P.; Kelly, S.M.; Mansfield, A. Permeability of silica monoliths containing micro- and nano-pores. *J. Porous Mater*, **2011**, *18*, 501-508.

Figure S1. SEM images of the three calcium carbonate powders used here: FC10 (left), FC30 (middle) and FC200 (right). The scale bar represents a length of 20 μm.

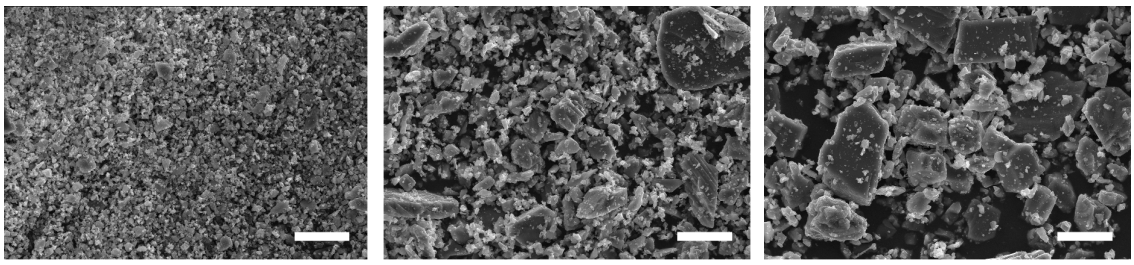

Figure S2. Upper plot: variation of pressure drop (between pressure gauge 1 and column exit) with volumetric flow rate for water pumped through packed columns containing either zero calcite (but including frits), FC10, FC30 or FC200 respectively. Lower plot: variation of packed column average effective pore radius (r_{pore}, derived as described in the text) with the mean radius of the calcite particles packed in the column ($r_{particle}$). For FC10, both water and decane flow measurements were used to determine r_{pore}. The diagonal lines correspond to the linear scaling relationships: $r_{pore} = 0.114\ r_{particle}$ (upper line for FC10 with $r_{particle} = 1.4$ μm and $\phi_{pore} = 0.45$), $r_{pore} = 0.066\ r_{particle}$ (middle line for FC30 with $r_{particle} = 5.0$ μm and $\phi_{pore} = 0.40$) and $r_{pore} = 0.030\ r_{particle}$ (lower line for FC200 with $r_{particle} = 23$ μm and $\phi_{pore} = 0.34$).

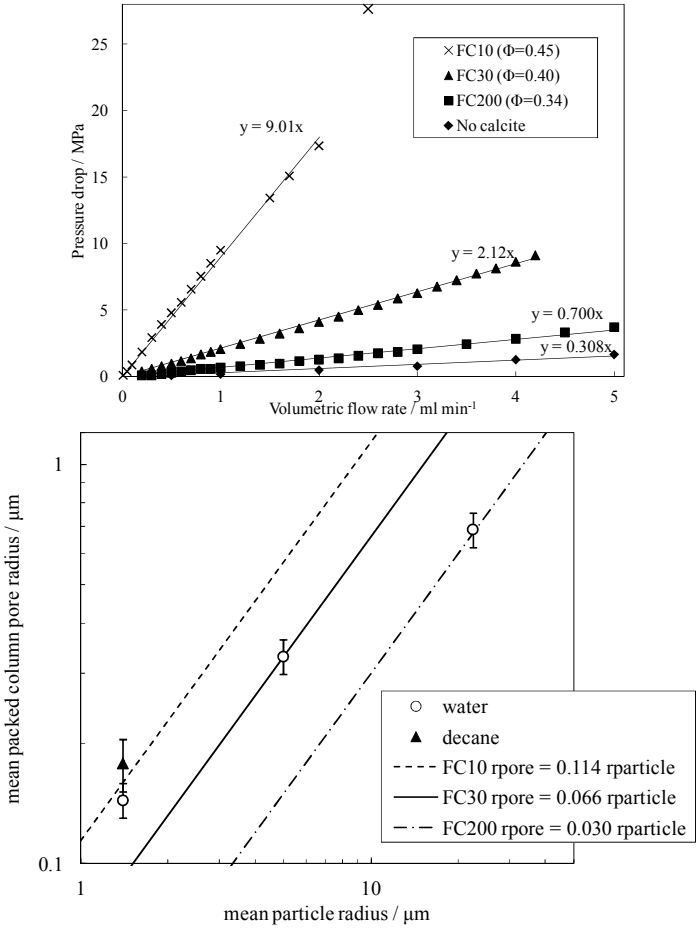

Figure S3. Cumulative size distributions for the calcium carbonate powders obtained from sieve analysis (Manufacturer's information) and SEM images. The vertical solid lines indicate the mean particle sizes corresponding to the averages of the sieve aperture size at 50% of the cumulative distributions and the mean sizes estimated from analysis of the SEM images.

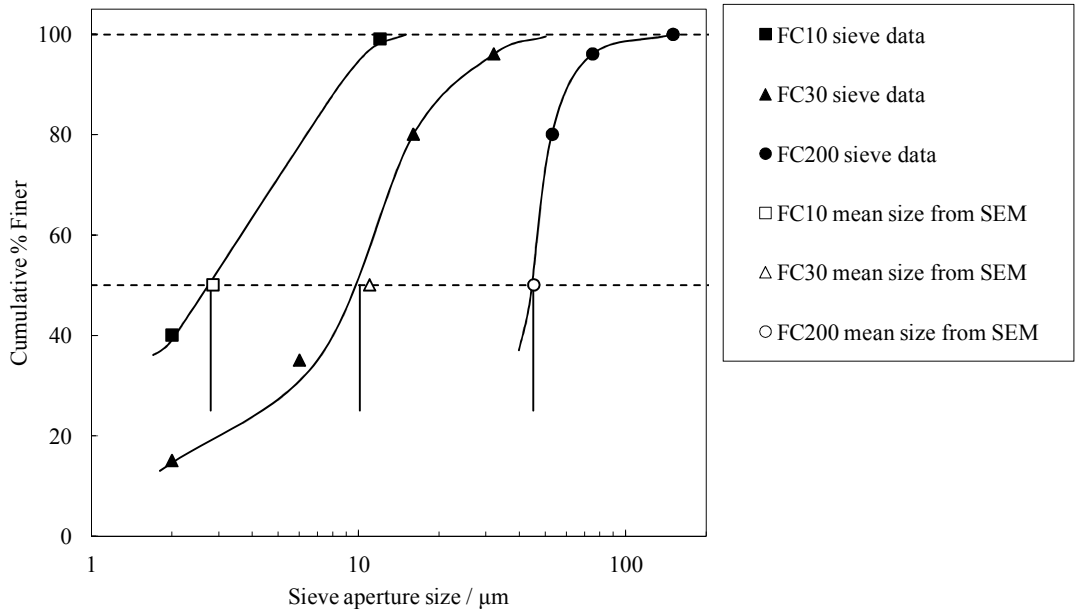

Figure S4. Examples of the variation of pressure drop with volume of liquid pumped. For each system, the figure legend includes the interfacial tension between the displacing and displaced fluid, the relevant contact angle, the estimated pressure drop required for liquid flow (ΔP_{flow}) and the estimated capillary pressure (ΔP_{cap}) calculated as either $2\gamma/r_{pore}$ or $2\gamma/r_{chan}$.

Figure S4a: variation of pressure drop (between pressure sensor 1 and column exit) with volume of decane pumped at 1 ml min^{-1} into an FC10 packed column with pore volume fraction 0.45 initially containing air. (Oil-air tension = 23.4 mN m^{-1}, contact angle through decane = 0^o, ΔP_{cap} = -0.29 to -0.080 MPa and ΔP_{flow} = 8.4 MPa)

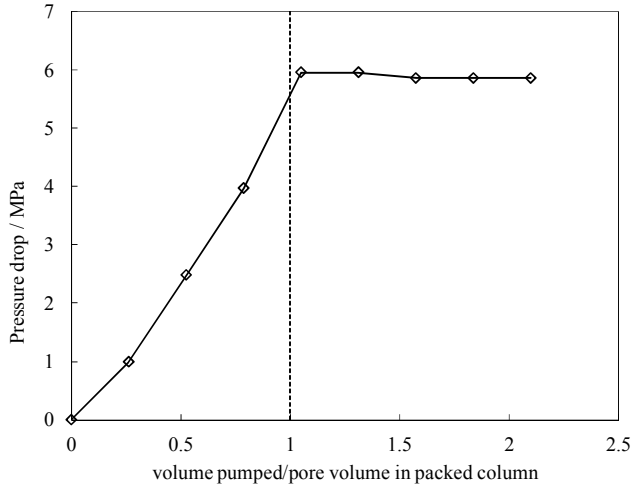

Figure S4b: variation of pressure drop (between pressure sensor 2 and column exit) with volume of decane pumped using syringe pump at 0.0083 ml min^{-1} into an FC10 packed column with pore volume fraction 0.45 initially containing air. (Oil-air tension = 23.4 mN m^{-1}, contact angle through decane = 0^o, ΔP_{cap} = -0.29 to -0.080 MPa, and ΔP_{flow} = 0.070 MPa.)

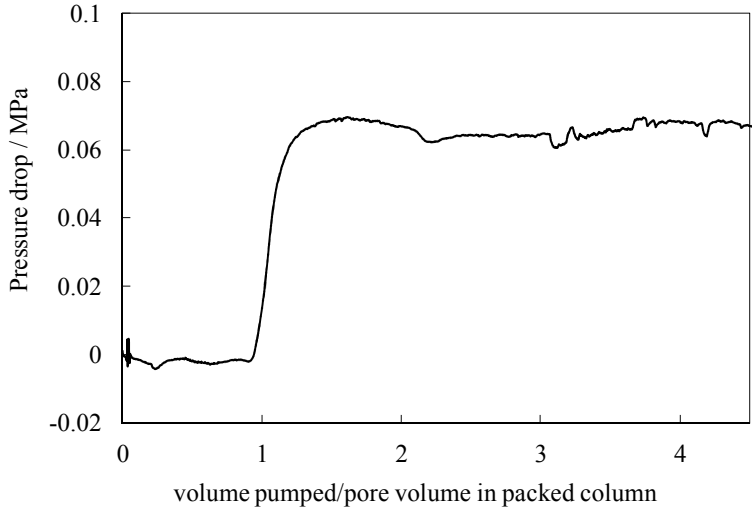

Figure S4c: variation of pressure drop (between pressure sensor 2 and column exit) with volume of water containing 0.1 mM AOT, 75 mM NaCl and 10 mM Na_2CO_3, pumped at 0.005 ml min^{-1} into an FC10 packed column with pore volume fraction 0.45 initially containing decane. (Oil-water tension = 7.1 mN m^{-1}, contact angle through water = 135°, ΔP_{cap} = 0.13 to 0.036 MPa and ΔP_{flow} = 0.044 MPa.) Note that the "noise" on the pressure plot corresponds to regular fluctuations caused by the piston stroke cycle of the HPLC pump used here.

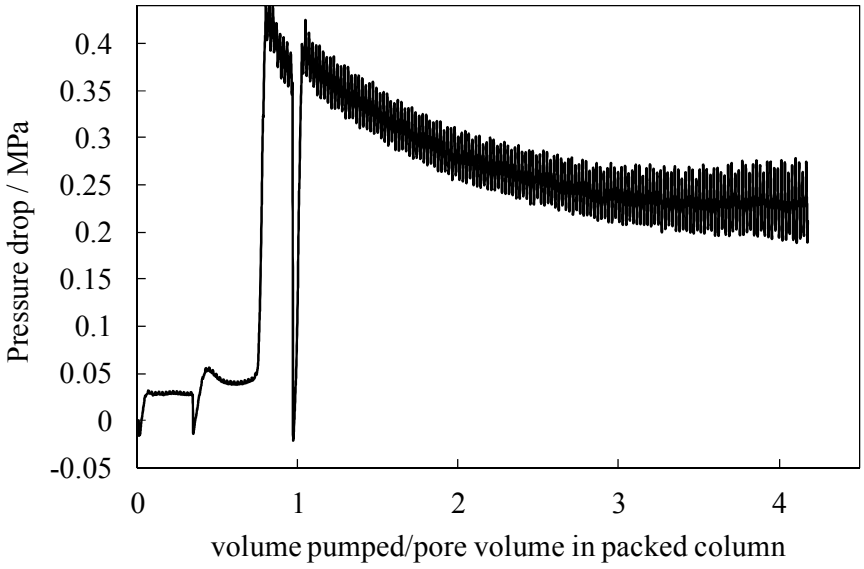

Figure S5. Upper plot: Variation of %oil recovery after 4 pore volumes versus flow rate for water (filled squares) and 10 mM AOT, 75 mM NaCl and 10 mM $Na_2 CO_3$ (crosses) pumped into an FC10 packed column initially containing decane. The lower plot shows the same oil recovery data plotted versus capillary number.

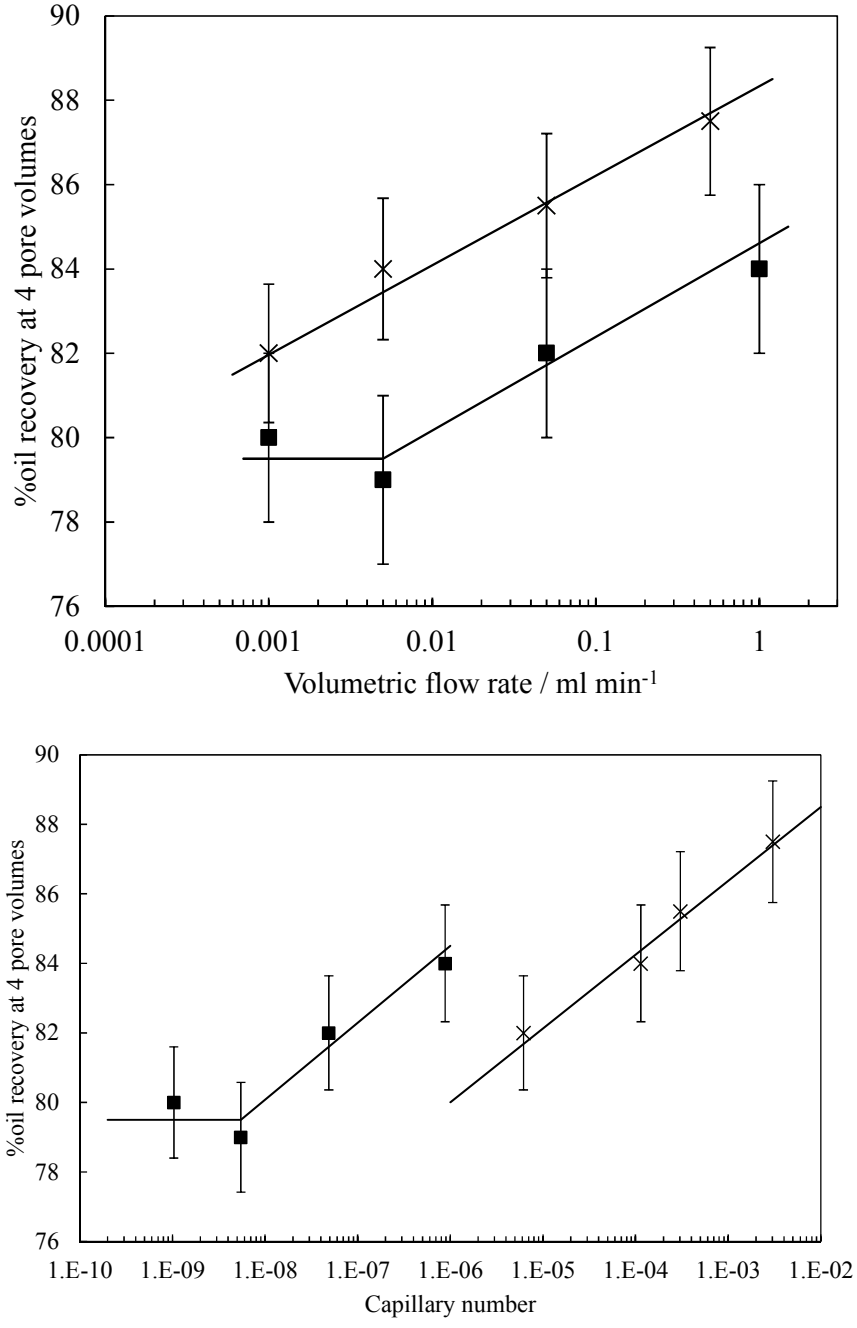

Figure S6. Variation of %oil recovered after 4 pore volumes as a function of the non-adsorbed (free) AOT concentration for solutions containing 0 mM NaCl and 10 mM Na_2CO_3. The vertical black dashed line shows the cmc and the horizontal black dashed line indicates the %oil recovered in the absence of AOT. The red dashed line shows the %oil recovered from the contact angle alone mechanism, and the green dotted line the %oil recovered from the contact angle and the solubilisation/emulsification mechanisms combined, both calculated using the model described in the text.